Supporting Information

Enhanced Performance of a Molecular Photoacoustic Imaging Agent by Encapsulation in Mesoporous Silicon Nanoparticles

Jinyoung Kang, Dokyoung Kim, Junxin Wang, Yunho Han, Jonathan M. Zuidema, Ali Hariri, Ji-Ho Park, Jesse V. Jokerst, and Michael J. Sailor*

[*]Corresponding author: msailor@ucsd.edu

This PDF file includes:

Materials
Supporting Figures: S1 to S15
Additional References

Materials
All chemical reagents were purchased from Aldrich Chemicals, Inc. Single crystal silicon wafers were obtained from Virginia Semiconductor, Inc. Indocyanine green (ICG) was purchased from Sigma-Aldrich Inc. (United States Pharmacopeia (USP) reference standard). Solid $CaCl_2$ was purchased from Spectrum Chemicals, Inc. 1,2-dimyristoyl-sn-glycero-3-phosphocholine (DMPC) and 1,2-distearoyl-sn-glycero-3-phosphoethanolamine-N-[methoxy(polyethylene glycol)-2000] (ammonium salt) (DSPE-PEG(2000) methoxy) were purchased from Avanti Polar Lipids, Inc. Sephadex G-50 beads were purchased from GE Healthcare Life Sciences, Inc. 100 kDa dialysis tubing (biotech cellulose ester membrane) was purchased from Spectrum Lab, Inc. Amicon 100 kDa centrifugal filter units were purchased from Millipore Sigma, Inc. 120 nm microporous silica nanospheres were purchased from Nanocomposix, Inc.
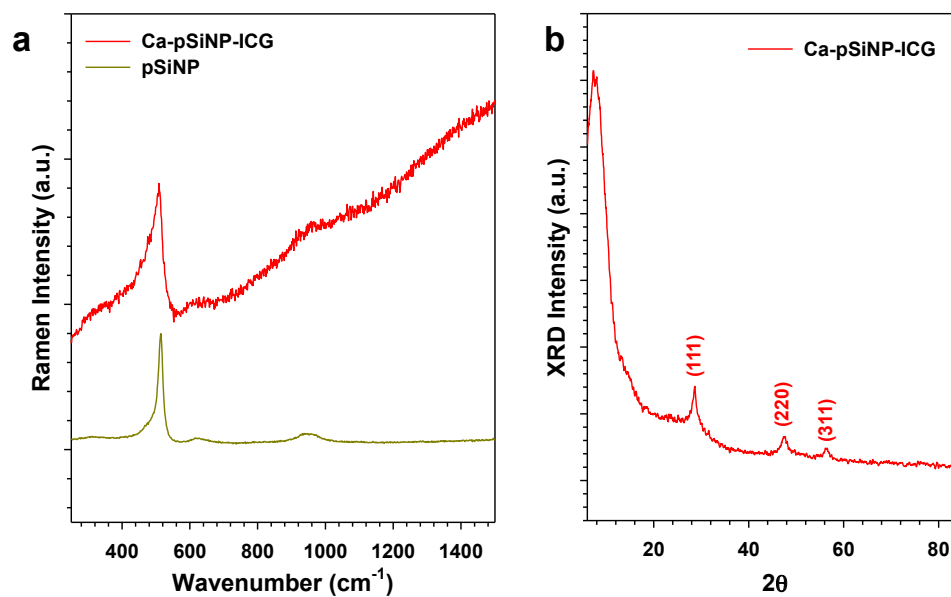
Supporting Figures

Figure S1. (a) Raman spectrum of Ca-pSiNP-ICG and pSiNP. (b) Power X-ray diffraction spectrum of Ca-pSiNP-ICG and pSiNP. The crystalline Si lattice planes based on Miller indices, *h k l*, are labeled in the diffraction pattern.
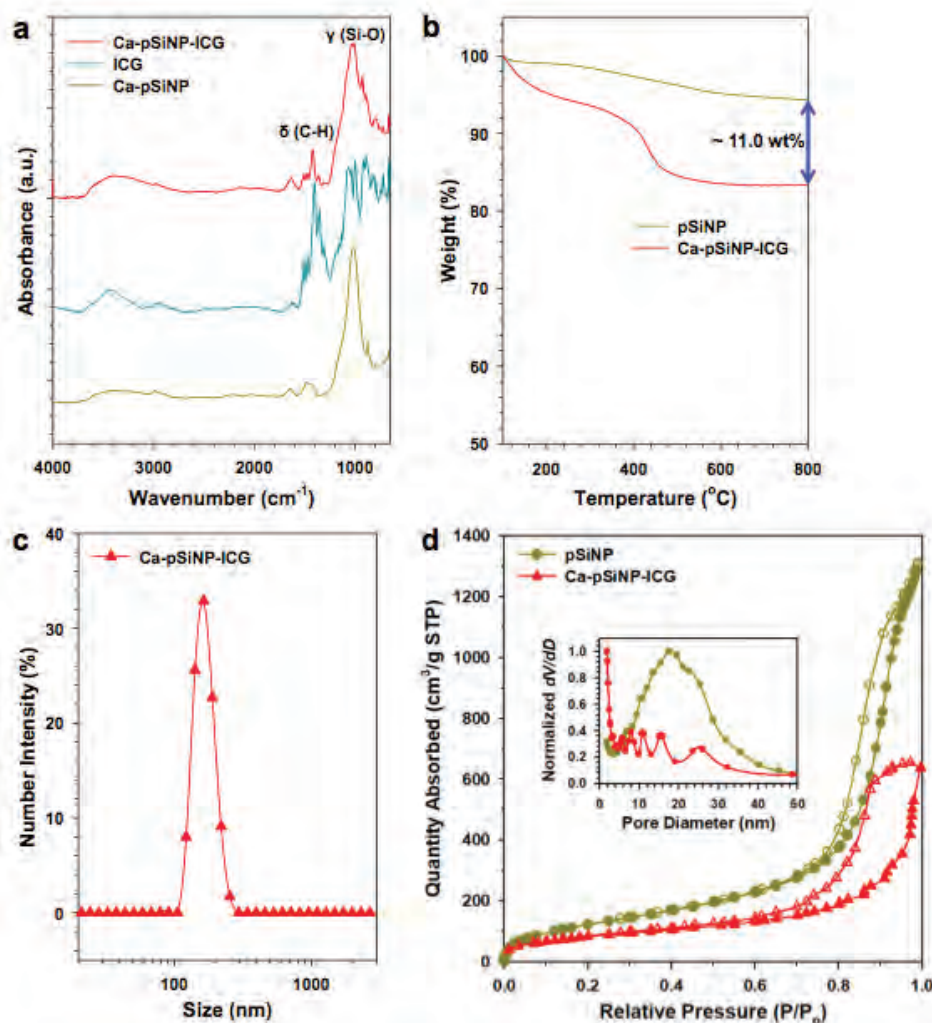
Figure S2. (a) ATR-FTIR spectra of Ca-pSiNP-ICG, ICG, and Ca-pSiNP (top to bottom). Si-O stretching (1000 cm⁻¹) and C-H bending (1420 cm⁻¹) modes are assigned (Symbol: ν = stretching, δ = bending). Spectra are offset along the y-axis for clarity. (b) Thermogravimetric analysis (TGA) data of pSiNP and Ca-pSiNP-ICG. The particles were fully dried for 4 h in a vacuum oven prior to analysis. The weight change (%) is plotted from 100 to 800 °C. The difference of net weight change between pSiNP and Ca-pSiNP-ICG is ~11 %, as indicated in the graph. (c) Size distribution of Ca-pSiNP-ICG in ethanol measured by dynamic light scattering (DLS). (d) Cryogenic nitrogen adsorption-desorption isotherms and pore size distribution (inset) of pSiNP starting material and Ca-pSiNP-ICG as indicated.
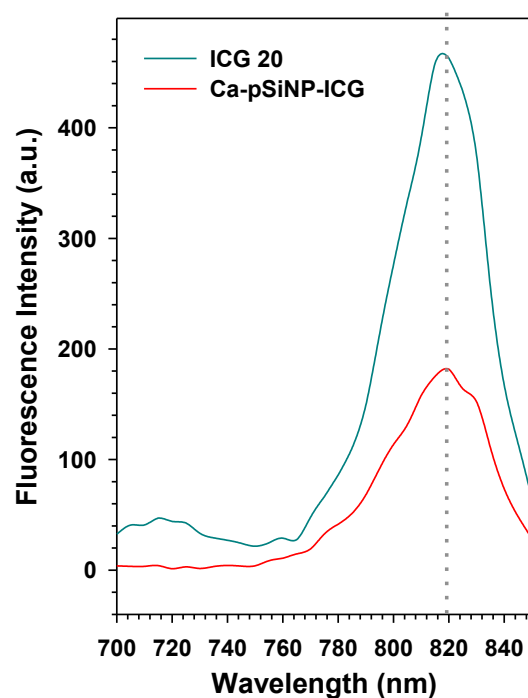
3

Figure S3. Fluorescence spectra of free ICG (ICG 20) and Ca-pSiNP-ICG in ethanol. The concentration of ICG in the ICG 20 sample was 20 µg/mL, and the concentration of the Ca-pSiNP-ICG sample was adjusted such that it displayed the same optical absorbance value at λ_{abs} = 790 nm. The emission spectra show maxima at λ_{em} = 820 nm, indicated by the gray dotted line.
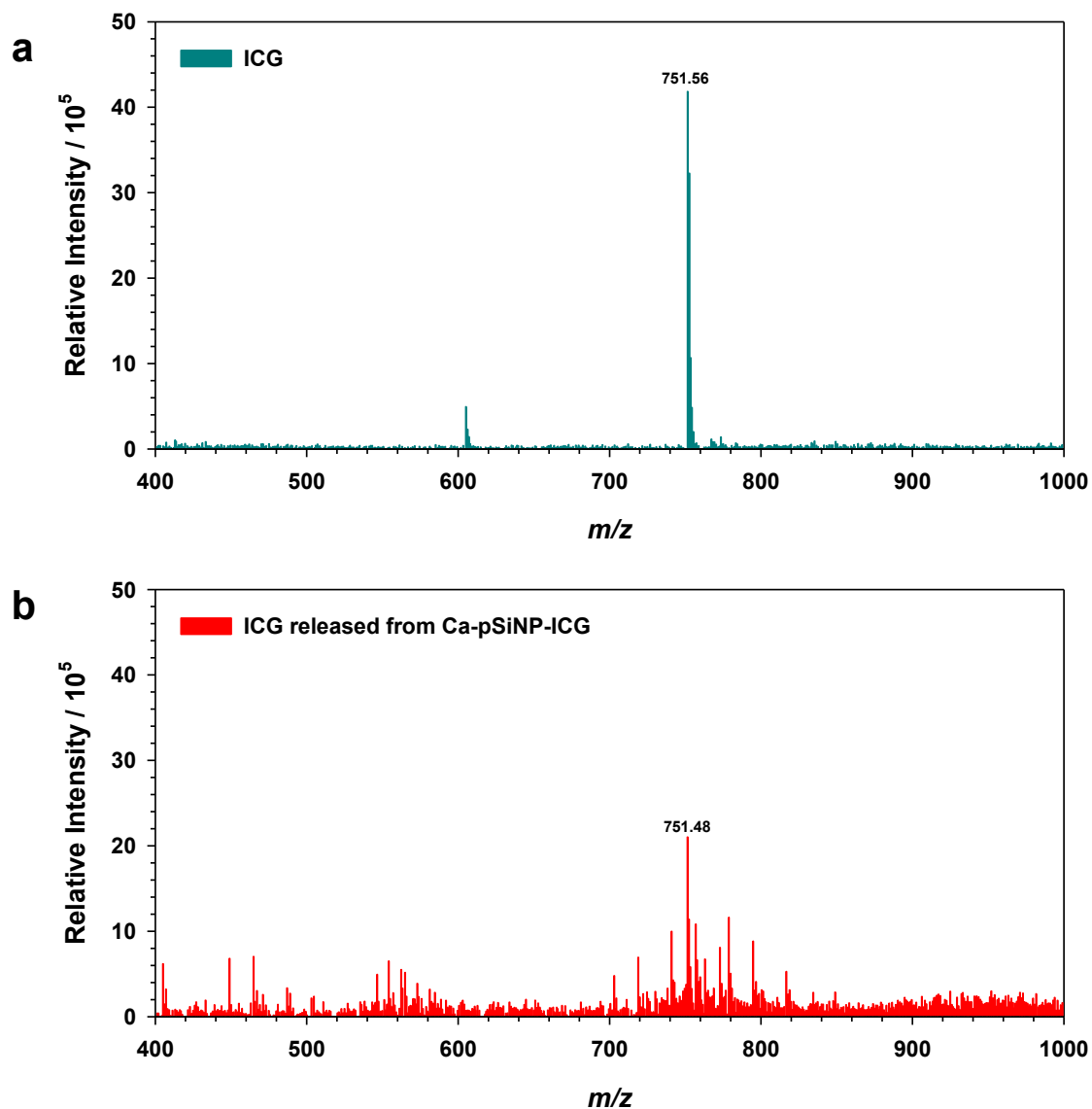
Figure S4. The electrospray ionization mass spectrometry (ESI-MS) of (a) ICG and (b) ICG released from Ca-pSiNP-ICG. Ca-pSiNP-ICG was dispersed in DI water (1 mg/mL) for 24 h to dissolve the pSiNP host and release loaded ICG, and the supernatant was collected by centrifugation (14,000 rpm, 20 min). The supernatant was diluted with methanol (10 % DI water in methanol), and the ESI-MS spectrum was obtained in negative ion mode. The characteristic mass of the parent ion at m/z = 751 was observed in both ICG control (a) and in the supernatant (b).
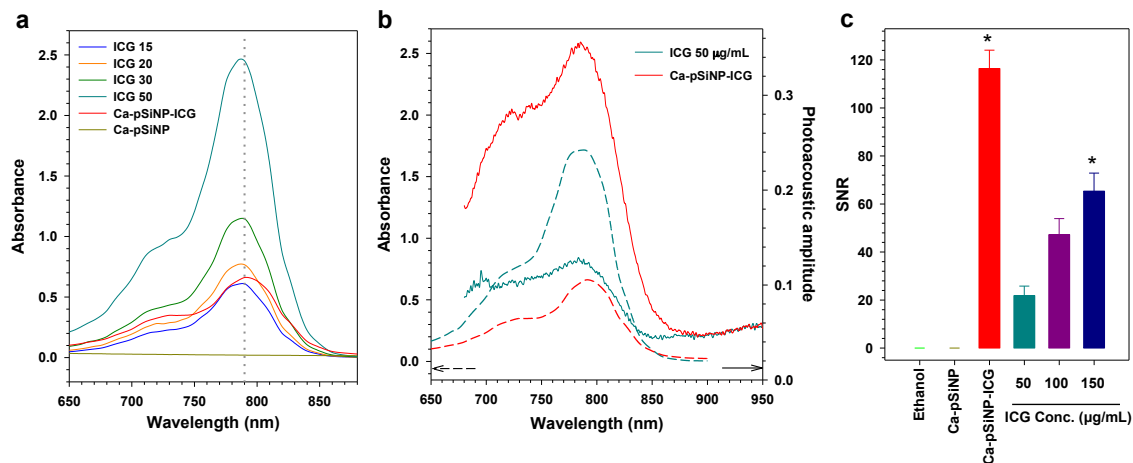
Figure S5. Photoacoustic performance of Ca-pSiNP-ICG relative to controls. (a) Optical absorbance spectra (in ethanol) of free ICG, Ca-pSiNP-ICG, and Ca-pSiNP (control containing no ICG). The number designations after "ICG" in the legend indicates the concentration of ICG in the solution (15, 20, 30, 50 µg/mL). Ca-pSiNP has no absorbance at 790 nm, which is indicated with gray dotted line. (b) UV-Vis absorbance (dashed line) and photoacoustic amplitude (solid line) spectra of ICG (50 µg/mL, cyan color) and Ca-pSiNP-ICG (red color). The absorption at 790 nm is obtained (a) prior to acquisition of the photoacoustic spectra. (c) SNR of photoacoustic signal from ethanol, Ca-pSiNP, Ca-pSiNP-ICG, and ICG 50, 100, 150 µg/mL (*$p < 0.01$). SNR obtained using Image J software.
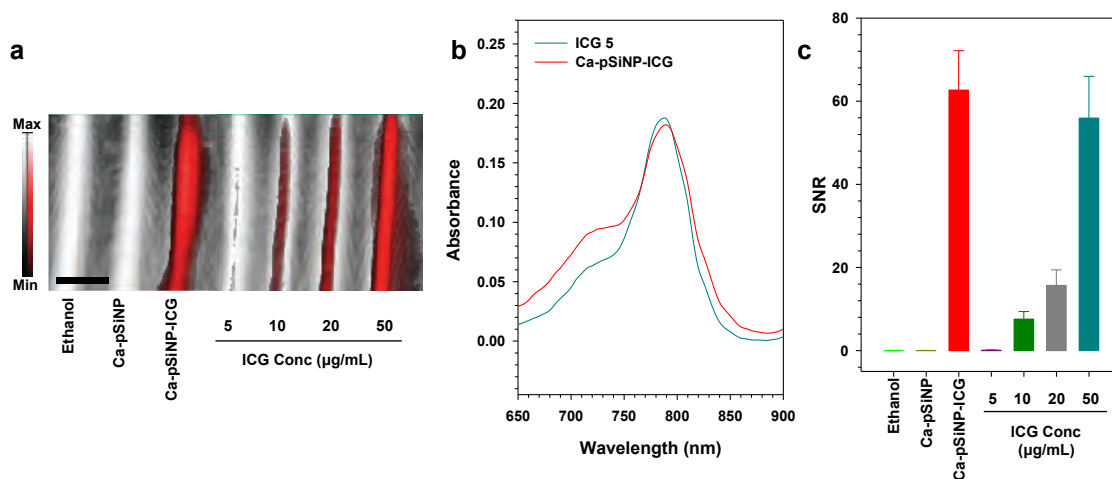
Figure S6. Photoacoustic performance of Ca-pSiNP-ICG tested at lower concentrations and compared with controls. (a) Photoacoustic imaging data overlaid on ultrasound image. Tubes contain (from left to right): pure ethanol, Ca-pSiNP (nanoparticles not containing ICG), Ca-pSiNP-ICG (containing total of 5 ug/mL ICG), and free ICG at the concentrations indicated. Solvent for all samples is pure ethanol. Scale bar is 3 mm. (b) UV-Vis absorbance spectra of free ICG (5 μg/mL) and Ca-pSiNP-ICG in ethanol. (c) SNR of photoacoustic signals from (a). SNR was obtained using Image J software.

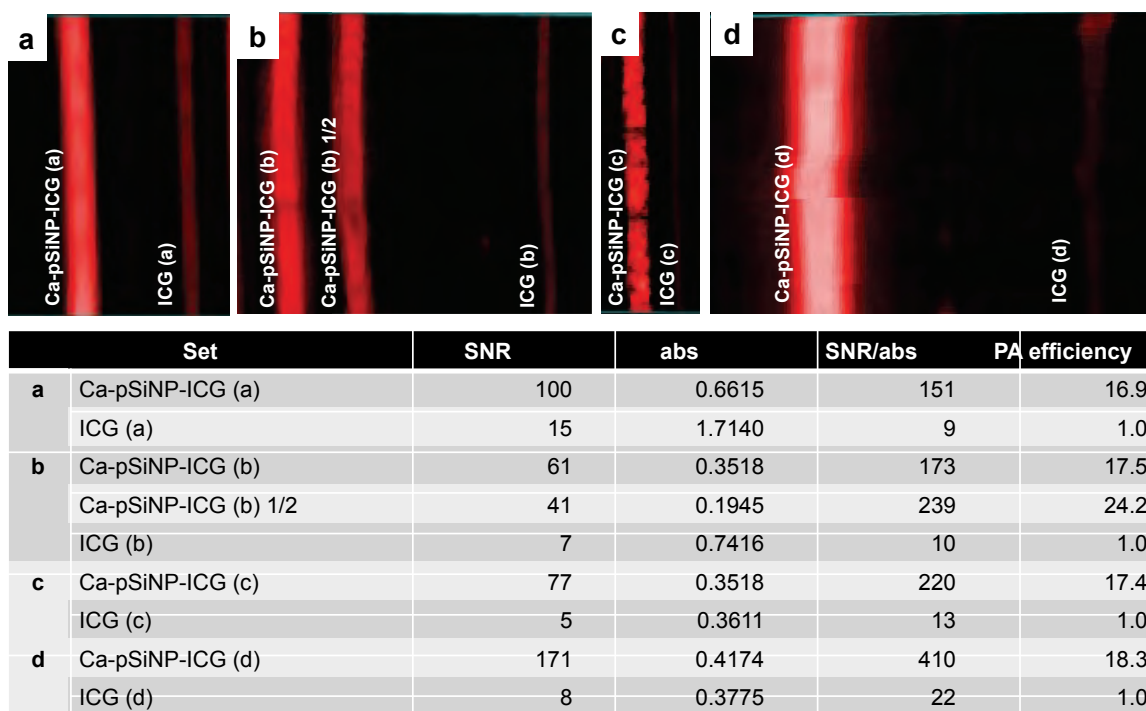|	Set	SNR	abs	SNR/abs	PA efficiency
a	Ca-pSiNP-ICG (a)	100	0.6615	151	16.9
	ICG (a)	15	1.7140	9	1.0
b	Ca-pSiNP-ICG (b)	61	0.3518	173	17.5
	Ca-pSiNP-ICG (b) 1/2	41	0.1945	239	24.2
	ICG (b)	7	0.7416	10	1.0
c	Ca-pSiNP-ICG (c)	77	0.3518	220	17.4
	ICG (c)	5	0.3611	13	1.0
d	Ca-pSiNP-ICG (d)	171	0.4174	410	18.3
	ICG (d)	8	0.3775	22	1.0

Figure S7. Replicates comparing PA response of Ca-pSiNP-ICG with free ICG. (a) Image taken from the photoacoustic image of Figure 1f showing the Ca-pSiNP-ICG and ICG 15 µg/mL tubes. (b) Photoacoustic image taken from Figure S10b showing the Ca-pSiNP-ICG and free ICG 10 µg/mL tubes. (c, d) Photoacoustic images of replicate Ca-pSiNP-ICG and free ICG samples. Table at the bottom lists SNR, absorbance, SNR/absorbance ratio and PA efficiency values from samples a-d. The PA efficiency was normalized to the measured value for ICG in each set. SNR was obtained using Image J software. Absorbance was obtained by UV-Vis plate reader using 100 µL volume.
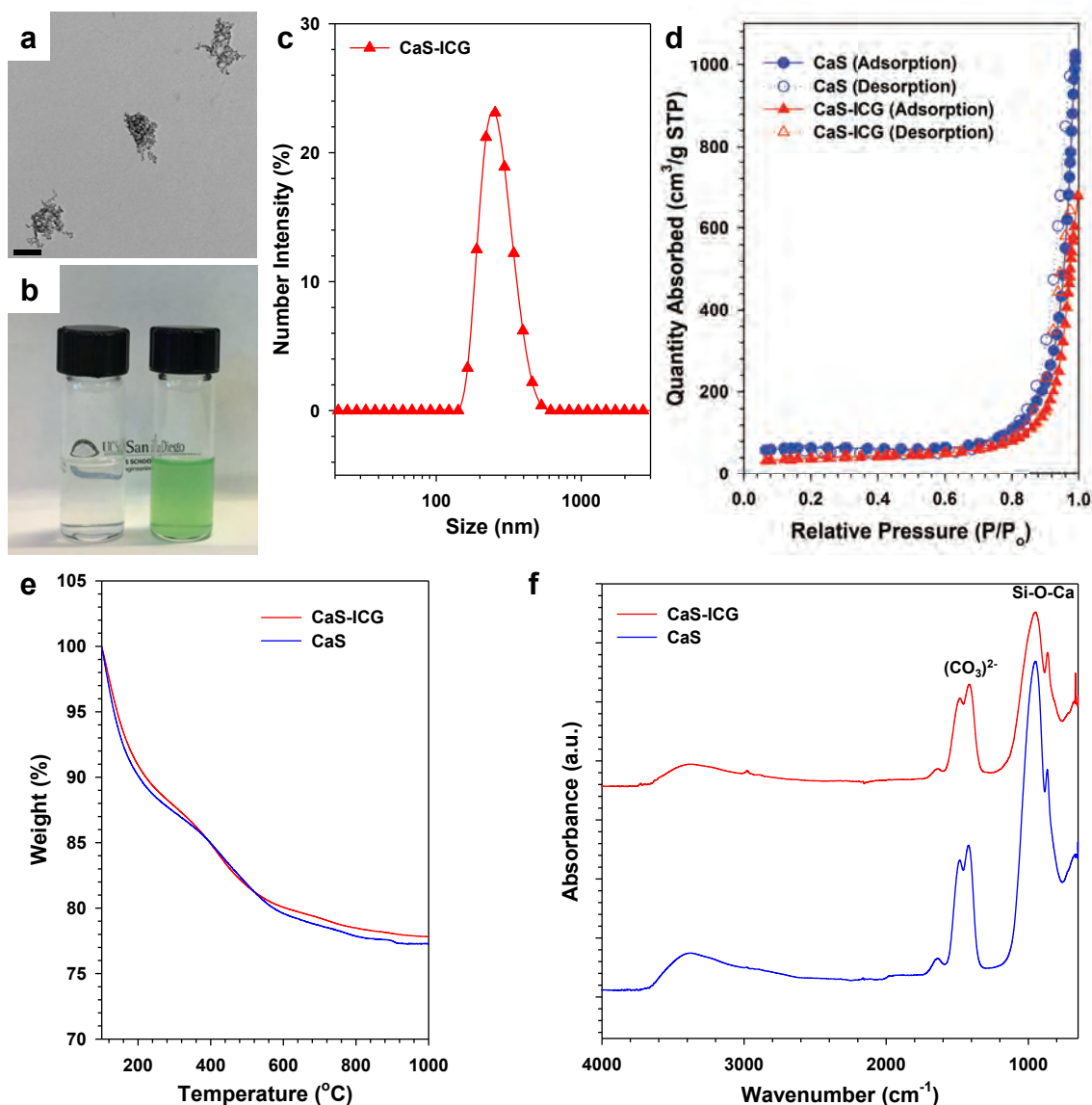
Figure S8. (a) Transmission electron microscope (TEM) image of ICG-loaded calcium silicate nanoparticles (CaS-ICG). (b) Photograph of calcium silicate nanoparticles without ICG loading (left) and calcium silicate nanoparticles with ICG loading (right). (c) Size distribution of CaS-ICG in ethanol measured by dynamic light scattering (DLS). (d) Cryogenic nitrogen adsorption-desorption isotherms for CaS and CaS-ICG. (e) TGA data of CaS and CaS-ICG. The particles are fully dried for 4 h in the vacuum oven prior to analysis. The difference of weight change (%) between CaS and CaS-ICG was negligible (< 0.6%). ICG seems to replace some portion of CaS skeleton during loading reaction. (f) ATR-FTIR spectra of CaS-ICG and CaS (top to bottom). Characteristic peaks of ICG (near 1420 cm^{-1}) are not obvious due to the large signals from calcium silicate (Si-O-Ca 950 cm^{-1}, $(CO_3)^{2-}$ 1410-1490 cm^{-1})[1]. Spectra are offset along the y-axis for clarity.
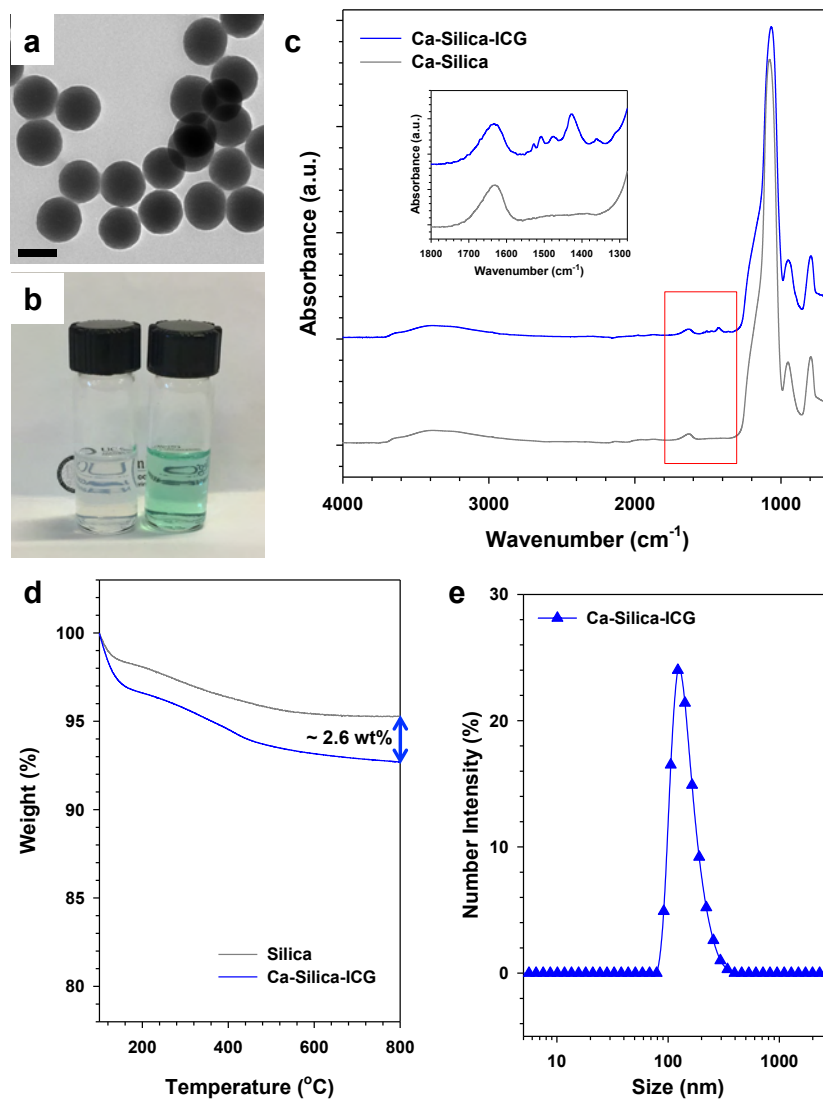
9

Figure S9. (a) Transmission electron microscope (TEM) image of ICG-loaded silica nanoparticles sealed with calcium silicate (Ca-Silica-ICG). (b) Photograph of calcium silicate-coated silica nanoparticles without ICG loading (Ca-Silica, left) and with ICG loading (Ca-Silica-ICG, right). (c) ATR-FTIR spectra of Ca-Silica-ICG and Ca-Silica (top to bottom). Inset is the expanded spectra in the region of 1300-1800 cm^{-1} to clarify the characteristic peaks of ICG (near 1420 cm^{-1}). Spectra are offset along the y-axis for clarity. (d) Size distribution of Ca-Silica-ICG in ethanol measured by DLS. (e) TGA data of Silica and Ca-Silica-ICG. The particles are fully dried for 4 h in the vacuum oven prior to analysis. The weight change (%) is plotted from 100 to 800 °C. The difference of net weight change between Silica and Ca-Silica-ICG is about 2.6 wt%, as indicated in the graph. (e) Size distribution of Ca-Silica-ICG in ethanol measured by DLS.
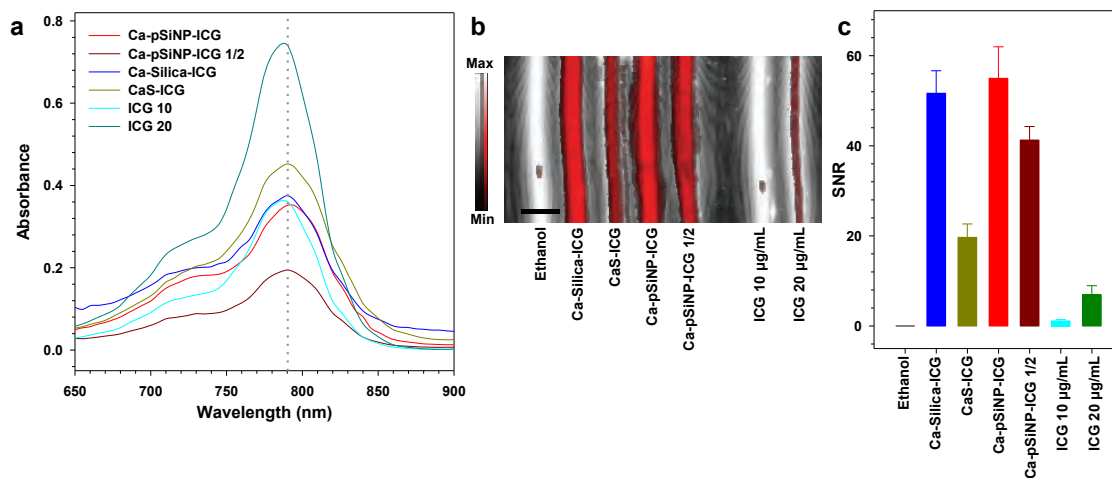
Figure S10. (a) UV-Vis absorbance of Ca-pSiNP-ICG, 2 times diluted Ca-pSiNP-ICG (Ca-pSiNP-ICG ½), Ca-Silica-ICG, CaS-ICG, ICG 10 and 20 μg/mL in ethanol. Absorption level at 790 nm (gray dotted line) of 3 different nanoparticles was lower than that of ICG 20 μg/mL, and compatible to ICG 10 μg/mL. (b) Photoacoustic image overlaid on ultrasound image. Each tube contains ethanol, Ca-Silica-ICG, CaS-ICG, Ca-pSiNP-ICG, Ca-pSiNP-ICG ½, ICG 10, and 20 μg/mL. Scale bar is 3 mm. (c) SNR of photoacoustic signals from (b). SNR was obtained using Image J software.
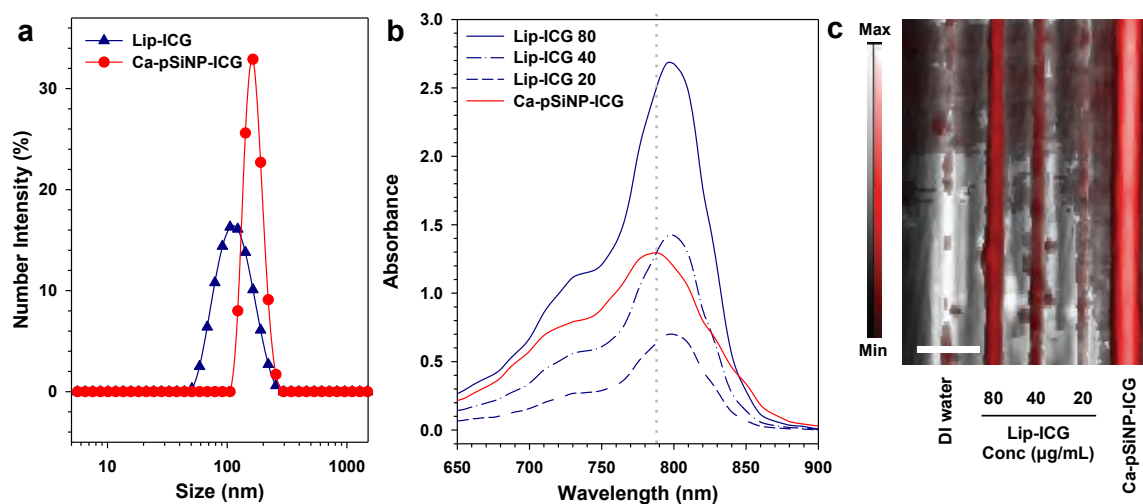
Figure S11. Properties of liposomal nanoparticles containing ICG (Lip-ICG), compared with the Ca-pSiNP-ICG construct. (a) Size distribution of Lip-ICG (blue triangles) and Ca-pSiNP-ICG (red circles) measured by dynamic light scattering (DLS). Lip-ICG and Ca-pSiNP-ICG samples were measured in DI water and ethanol, respectively. (b) Optical absorbance spectra of Lip-ICG containing 80, 40, and 20 μg/mL ICG in DI water, and Ca-pSiNP-ICG in ethanol. The Lip-ICG 40 and Ca-pSiNP-ICG formulations showed the same absorbance at λ = 788 nm as indicated (gray dotted line). (c) Photoacoustic response of Ca-pSiNP-ICG and Lip-ICG. Photoacoustic image overlaid on ultrasound image with a maximum intensity projection. Each tube contains DI water, liposomal formulations of ICG (Lip-ICG) containing 80, 40, and 20 μg/mL of ICG in DI water, and Ca-pSiNP-ICG in pure ethanol.
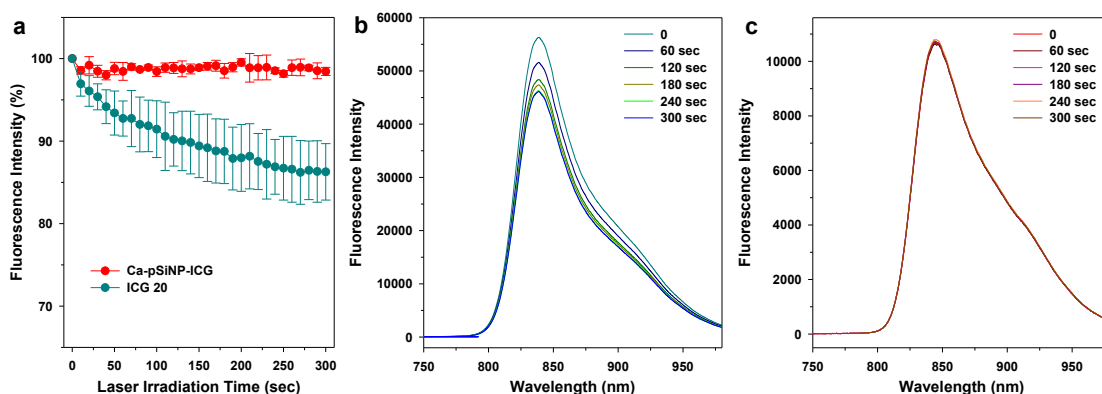
Figure S12. Comparison of fluorescence intensity of ICG and Ca-pSiNP-ICG under laser irradiation over time. (a) Normalized fluorescence intensity (integrated over λ_{em} = 800 - 980 nm) from free ICG and from Ca-pSiNP-ICG, obtained under pulsed laser irradiation (tripled YAG-pumped optical parametric oscillator, λ_{ex} = 790 nm, 20 Hz repetition rate, average power = 0.3 mW). Steady state fluorescence spectra were obtained every 10 sec using a QE Pro spectrometer (Ocean Optics) fitted with an 800 nm long-pass emission filter. The initial integrated fluorescence intensity value measured was set as 100% intensity at 0 sec. Fluorescence spectra were acquired every 10 sec, and the integrated intensity was normalized based on the 0 sec value (n = 3). (b, c) Family of raw fluorescence spectra of free ICG (b) and the Ca-pSiNP-ICG formulation (c) obtained during laser irradiation. The temperature increase measured after 300 sec of laser irradiation in this experiment was 7 ± 1 °C for ICG and 21 ± 3 °C for Ca-pSiNP-ICG, measured by infrared thermometer. Optical absorbance measured from both samples before the experiment was equivalent.
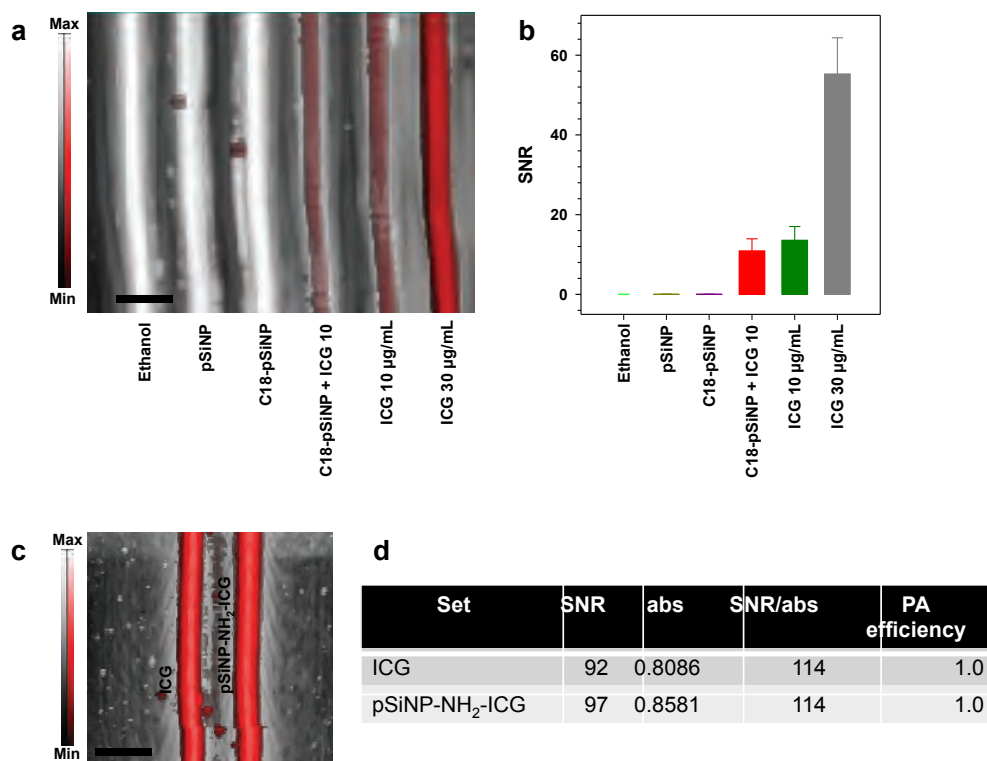
Set	SNR	abs	SNR/abs	PA efficiency
ICG	92	0.8086	114	1.0
pSiNP-NH$_2$-ICG	97	0.8581	114	1.0

Figure S13. Photoacoustic response of chemically modified pSiNPs, where the pores have been either blocked by grafting of octadecyl (C18) chains, or modified with amine groups in order to display a net positive surface charge. (a) Photoacoustic image overlaid on ultrasound image. Tubes contain (from left to right): pure ethanol, pSiNP, C18-pSiNP, C18-pSiNP + ICG 10, free ICG 10, and 30 µg/mL. C18-pSiNP + ICG 10 indicates a 1:1 (by volume) mixture of C18-pSiNP (1 mg/mL) and ICG (20 µg/mL); final ICG concentration was 10 µg/mL. ICG 10 µg/mL indicates a 1:1 (by volume) mixture of pure ethanol and ICG (20 µg/mL); final ICG concentration was 10 µg/mL. Scale bar is 3 mm. (b) Signal to noise ratio (SNR) of photoacoustic data from (a). Sample identity as indicated in (a). SNR was obtained using Image J software. (c) Photoacoustic response of amine-functionalized pSiNPs containing electrostatically bound ICG (pSiNP-NH$_2$-ICG), compared to free ICG. The surface of the pSiNPs was modified using (3-aminopropyl)-dimethylmethoxysilane, and ICG was loaded *via* electrostatic surface interaction. (d) Comparison of the photoacoustic efficiency of free ICG with the electrostatically loaded pSiNP-NH$_2$-ICG formulation. SNR was obtained from the image of (c) using Image J software. The optical absorbance at $\lambda = 790$ nm is given in "abs", and it was measured from a 100 µL sample volume by plate reader. The "SNR/abs" column reports the ratio of SNR to absorbance at $\lambda = 790$ nm. The "PA efficiency" column gives the relative efficiency of photoacoustic signal generation, which is normalized to the SNR/abs value of free ICG. Within the error of the measurement, the ICG and pSiNP-NH$_2$-ICG samples showed no significant difference in PA generation efficiency.

a

b

- Fixed brain using PFA 4%
- Inject 15 µL solution
- PBS, ICG, Ca-pSiNP-ICG
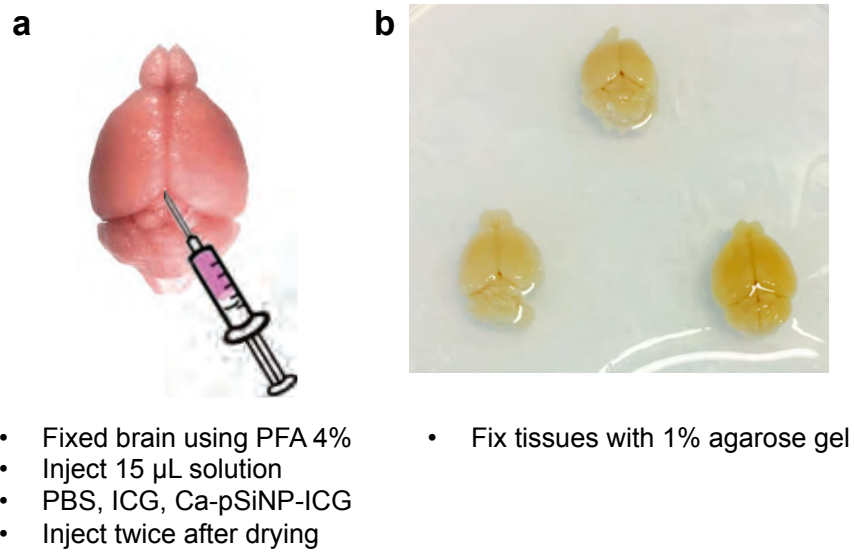- Inject twice after drying

- Fix tissues with 1% agarose gel

Figure S14. Schematic describing *ex vivo* brain preparation for photoacoustic imaging experiments. (a) Aliquots of PBS, ICG, or Ca-pSiNP-ICG were injected at the lambda point of the fixed brain tissue. Sample solutions were injected twice at an interval of 15 min. (b) Photograph of fixed brain tissues in 1% agarose gel.
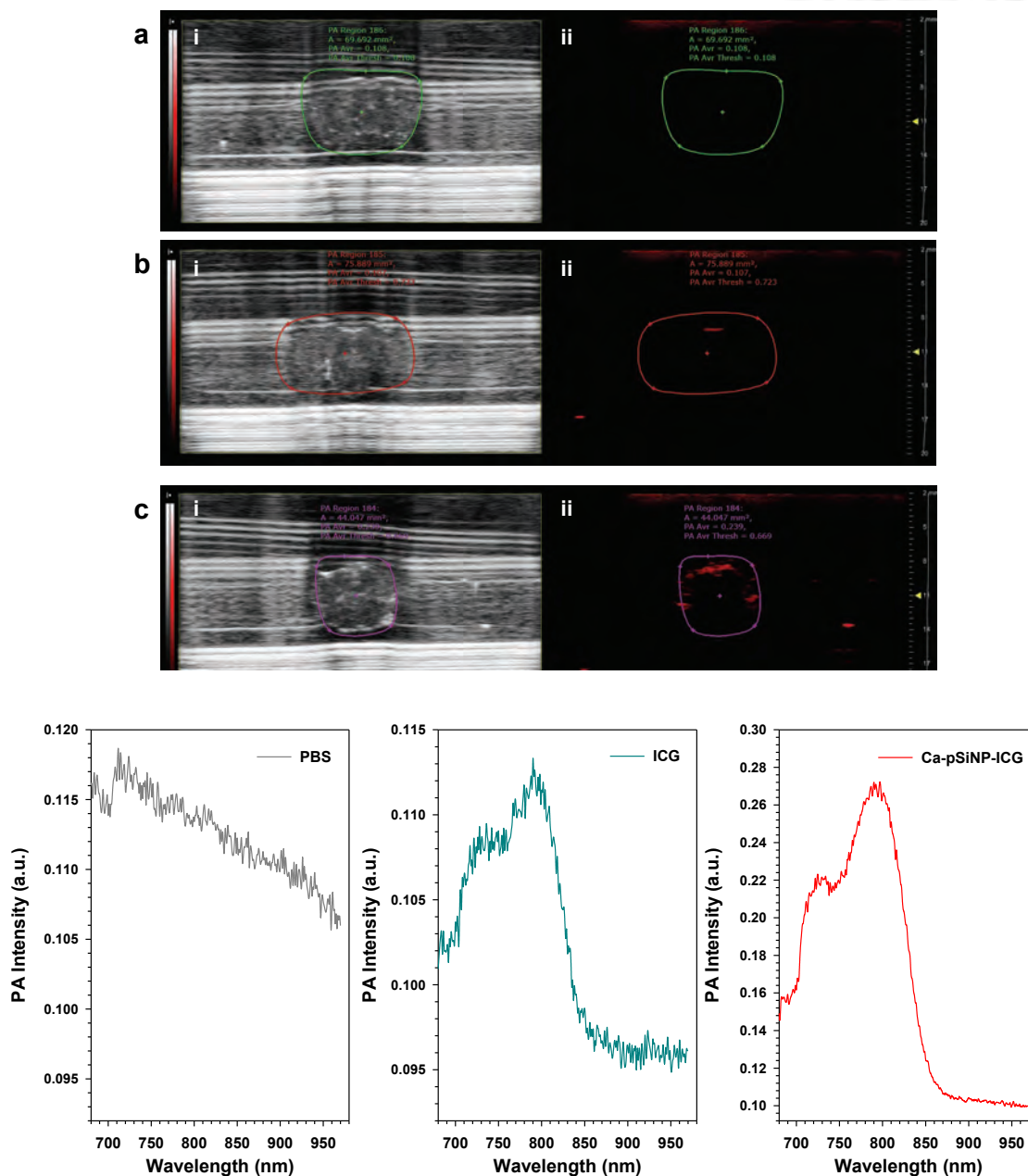
Figure S15. Images of brain coronal cross-sections after injection of (a) PBS, (b) free ICG, and (c) Ca-pSiNP-ICG. (i) Ultrasound image and (ii) photoacoustic image. The outlined margin indicates the region of interest for the photoacoustic spectra shown at the bottom (d-f). Photoacoustic spectra of (d) PBS, (e) ICG, and (f) Ca-pSiNP-ICG ICG injected brain tissue, obtained from brain coronal cross-sections in panels a, b, c, respectively.

16

WILEY-VCH

Reference

1. Baciu D, Simitzis J. Synthesis and characterization of a calcium silicate bioactive glass. *Journal of Optoelectronics and Advanced Materials* 2007, **9**(11)**:** 3320-3324.